Department of Spine Surgery and Musculoskeletal Tumor[1], Zhongnan Hospital of Wuhan University;
Department of Orthopedics[2], Wuhan Third Hospital, Wuhan City, People's Republic of China

Effects of different concentrations of metformin on osteoclast differentiation and apoptosis and its mechanism

Feng Bian[1], Yufeng Zhang[1], Yuanlong Xie[1], Hongyu Fang[2], Mingyu Fan[2], Xin Wang[2], Hongliang Li[2], Tao Huang[2], Sheng Zhang[1], Lin Cai[1,*]

Received February 2, 2021, accepted March 6, 2021

**Corresponding author: Lin Cai, Department of Spine Surgery and Musculoskeletal Tumor, Zhongnan Hospital of Wuhan University, Wuhan City, Hubei Province, 430071, People's Republic of China*
orthopedics@whu.edu.cn

Pharmazie 76: 244-248 (2021) *doi: 10.1691/ph.2021.1378*

This study aimed to investigate the effect of metformin on osteoclast differentiation and apoptosis. Low concentration of metformin inhibited osteoclast differentiation and downregulated the expression of TRAP, RANK, Cathepsink, NFATC-1, MMP-9 and TRAF-6. High concentration of metformin promoted osteoclast apoptosis and upregulated the expression of Bax/Bcl-2 and caspase-3; BV/TV, BS/TV, Tb.N and BMD were increased while Tp.Sp decreased in the group of intraperitoneal metformin+femoral intramedullary osteoclast injection (Met+OC) compared with the control group, 1 nM metformin downregulated Akt, p44/42 MAPK, JNK, p38 MAPK phosphorylation, 5 nM metformin down regulated ERK and Akt phosphorylation. These results suggest that a low concentration of metformin inhibits osteoclast differentiation through PI3K/Akt and MAPK/ERK signaling pathway; high concentrations of metformin promote osteoclast apoptosis through PI3K/Akt and ERK signaling pathway.

1. Introduction

Osteoclasts (OCs), which are tissue-specific macrophages with multiple nuclei, are generated by the differentiation of monocyte/macrophage precursor cells, and are considered as key players in bone remodeling. Most of the skeletal diseases in adults such as osteoporosis, periodontal disease, rheumatoid arthritis, multiple myeloma and bone metastasis of malignant tumors occur due to overactive osteoclast osteolysis, resulting in bone metabolic imbalances (Boyle et al. 2003). The incidence of osteoporosis and fracture risk are increased in patients with type 2 diabetes, while the risk of fracture is reduced under treatment with biguanides (Melton et al. 2008); Metformin (Met) plays a major role in reducing insulin resistance, but new functions are constantly being discovered, such as in the treatment of multiple sclerosis (Dziedzic et al. 2020). In addition, some studies have shown that Met might reduce the incidence of cancer in patients with type 2 diabetes mellitus (Libby et al. 2009). The overall survival rate of patients with colorectal cancer undergoing chemotherapy showed improvement (Bansal et al. 2011), and enabled patients with diabetes mellitus and breast cancer to attain better prognosis (Xu et al. 2015). However, the effect and mechanism of Met on osteoclasts are still unclear. Hence, this study aimed to investigate the effect of Met on osteoclast differentiation and apoptosis, and explore its possibility in treating osteoporosis and other bone loss diseases.

Abbreviations:
OCs, Osteoclasts; Met, metformin; BMMs, bone marrow mononuclear cells; PBS, phosphate buffered saline; MMP-9, matrix metalloproteinase-9; CTSK, Cathepsink; RANKL, receptor activator of nuclear factor kappa B ligand; M-CSF, macrophage colony-stimulating factor; NFATC-1, Nuclear transcription factor-activated T cell 1; AP-1, activator protein-1

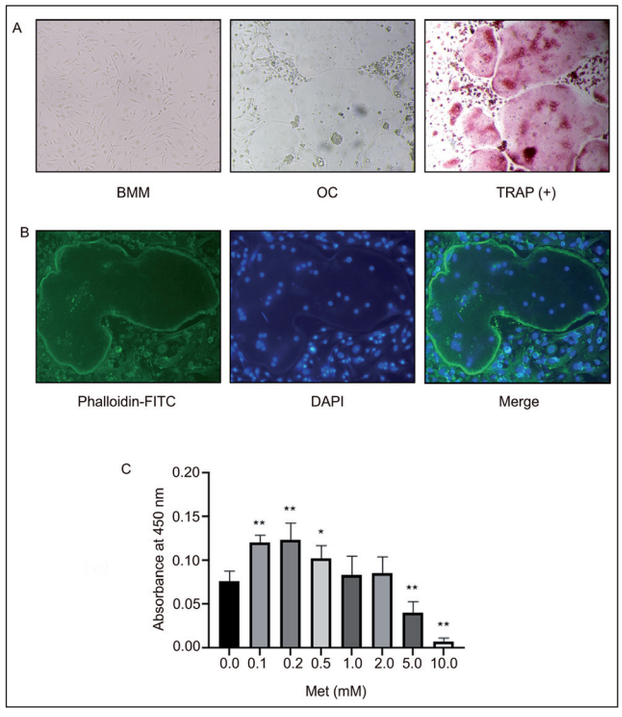

Fig. 1: Isolation and culturing of primary BMMs, induction of osteoclast differentiation, identification, and drug concentration screening. (a) light microscopy of primary BMMs at 100X, osteoclasts and TRAP staining; (b) the actin ring structure was observed under 200X light microscope with staining of phalloidin and DAPI; (c) BMMs were stimulated by Met for 48 hours, and the absorbance value was detected by CCK-8 method at 450nm. The data were expressed as means ± standard, * indicating $p < 0.05$, * * indicating $p < 0.01$.

2. Investigations and results

2.1. Isolation and culturing of primary BMMs, induction of osteoclast differentiation, identification and drug concentration screening

After induction of adherence, the primary BMMs appeared as long spindle shaped (Fig. 1a). After induction with 50 ng/ml M-CSF and 50 ng/ml RANKL for 6-8 days, the multinucleated giant cells that were surrounded by fibro-actin rings were fused, and the actin ring structure could be clearly displayed by phalloidin staining (Fig. 1b). TRAP positive cells with more than three nuclei were defined as osteoclasts (Fig. 1a). After 48 h of stimulation with Met, the proliferation of BMMs was not inhibited if the concentration of Met was less than 2 mM. At 5 mM and 10 mM, the proliferation of primary BMMs was significantly inhibited (Fig. 1c). Therefore, the range of 0-1 mM was selected for intervening the process of osteoclast differentiation, excluding the interference of false positives. Concentrations of 5 mM and 10mM were used to analyze the effect of Met on osteoclast apoptosis.

2.2. Low concentrations of Met inhibited osteoclast differentiation, while high concentrations of Met could promote osteoclast apoptosis

TRAP staining showed that Met (0.1, 0.2, and 1 mM) could inhibit osteoclast differentiation, and its inhibition was gradually increased with increasing concentration. Met (1 mM) completely inhibited osteoclastic differentiation induced by M-CSF and RANKL (Fig. 2a, b).

The results of bone resorption lacunae test showed that Met (0.1, 0.2, and 1 mM) effectively inhibited bone resorption of osteoclasts. With increasing the experimental concentration, the area of bone resorption lacunae showed a gradual decrease. At 1 mM concentration, no bone resorption lacuna was obvious anymore (Fig. 2c, d). Flow cytometry showed that osteoclasts had a certain tendency to self apoptosis, which was consistent with the phenomenon observed in the induction culture of osteoclasts. With increasing concentration of Met (5 mM,10 mM), the proportion of osteoclast apoptosis was shown to be gradually increased (Fig. 2e, f).

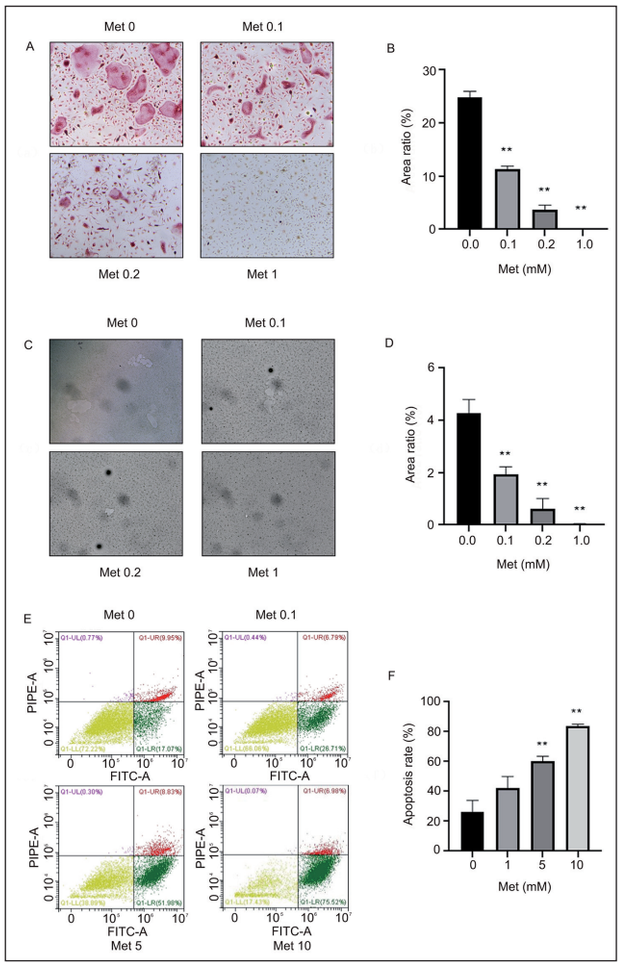

Fig. 2: Low concentration of metformin inhibits osteoclast differentiation; high concentration of metformin promotes osteoclast apoptosis. (A, B) TRAP staining was observed under a microscope at 100X; (C, D) bone resorption lacuna test was observed under a light microscope at 200X; (E, F) effect of metformin on osteoclast apoptosis as detected by flow cytometry. The data were expressed as means ± standard, * indicating $p < 0.05$, * * indicating $p < 0.01$.

2.3. Met inhibits the expression of osteoclast differentiation and apoptosis-related genes and proteins

Real-time PCR and Western blotting results showed that Met could inhibit the expression of TRAP, RANK, Cathepsink, NFATC-1, MMP-9, TRAF-6, and its inhibitory effect was gradually enhanced with increasing concentrations of Met and reached the strongest with 1 mM Met (Fig. 3a,c,d). However, the expression of Bax/Bcl-2 and caspase-3 was gradually increased when stimulated with 5 mM and 10 mM Met (Fig. 3 b,c,e).

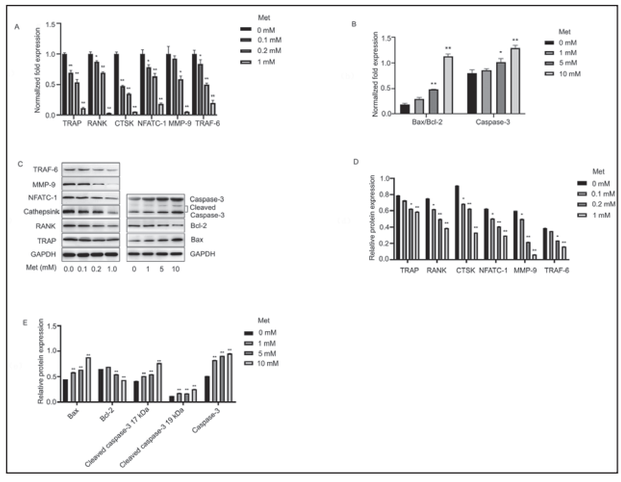

Fig. 3: Metformin inhibits the expression of osteoclast differentiation and apoptosis-related genes and proteins. (A)(B) Effect of metformin on osteoclast differentiation and apoptosis-related genes were detected by real-time PCR; (C) effects of metformin on osteoclast differentiation and apoptosis-related proteins and (D) (E) gray value data analysis. The data were expressed as means ± standard deviation, * indicating $p < 0.05$, * * indicating $p < 0.01$.

2.4. Met inhibits bone destruction of osteoclasts in nude mice

The results of micro CT showed that after injection of osteoclasts into the medullary cavity of the distal femur, the local bone mass showed enlargement, the epiphyseal line was destroyed, the shape was disordered, and the trabecular bone in the medullary cavity remained sparse. Otherwise, the bone destruction induced by osteoclasts was treated by intraperitoneal injection of Met. Data analysis results showed that the NS+OC group decreased bone surface area tissue volume ratio (BS/TV), trabecular number (TB. N), bone mineral density (BMD), and increased separation of trabecular bone (Tp.Sp). Also the three-dimensional reconstruction showed a similar effect. However, BS/BV and Tb.Th showed no statistical difference when compared with control group, suggesting that osteoclasts had no influence on TB.N during the study period. Compared with the control group, BV/TV, BS/TV, BS/BV, Tb.N, TP.SP, Tb.Th and BMD of the Met+NS group showed no statistical differences. However, the Met+OC group had higher BV/TV, BS/TV, Tb.N, BMD, and TP.Sp were decreased, suggesting that Met inhibited osteocatabolism of osteoclasts. Three-dimensional reconstruction showed similar effects. However, BS/BV and Tb.Th showed no statistical differences when compared with NS+OC group (Fig. 4a, b, c).

Immunohistochemical results of paraffin sections suggested that the number of TRAP positive cells in Met+NS group was significantly reduced, and the expression level of caspase-3 in osteoclasts was significantly increased. Otherwise, TRAP positive cells showed significant reduction and caspase-3 positive cells were increased in the Met+OC group when compared with control group NS+OC. These results suggested that the concentration of 200 mg/kg of Met *in vivo* had dual effects, and not only inhibits osteoclast differentiation, but also promotes osteoclast apoptosis (Fig. 4 d, e, f).

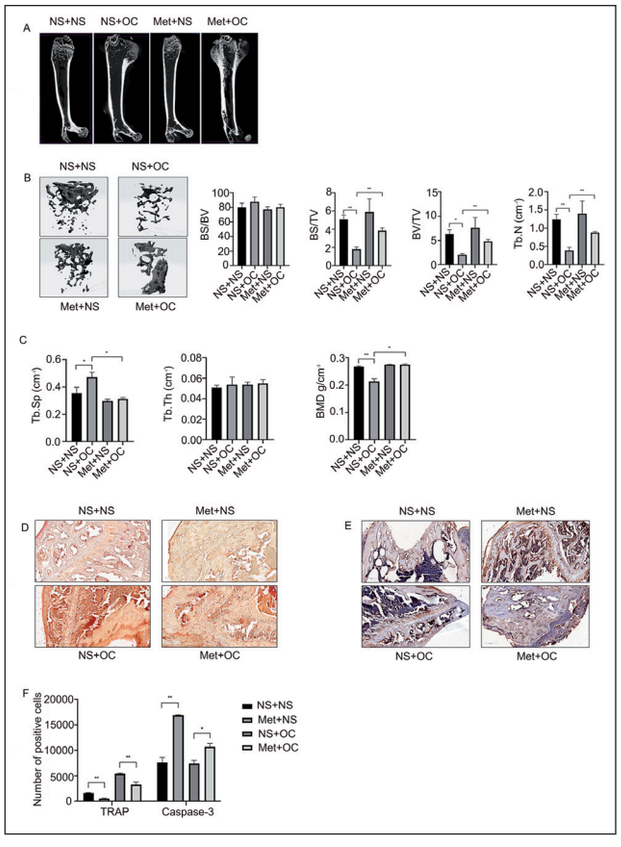

Fig. 4: Metformin inhibits bone destruction of osteoclasts in nude mice. (A) Full-length images of femurs were reconstructed in nude mice; (B) 3D reconstruction of images of trabeculae; (C) VOI regional data analysis of distal femur; (D) (E) (F) the number of TRAP and Caspase-3 positive cells in distal femoral and statistical analysis, Scale bar = 200μm. The data were expressed as means ± standard, * indicating $p < 0.05$, * * indicating $p < 0.01$.

2.5. Met regulates osteoclast differentiation and apoptosis through PI3K/Akt signaling pathway, MAPK/ERK signaling pathway and ERK signaling pathway

Western blotting analysis showed that phosphorylation of AKT, p44/42 MAPK, JNK, and p38 MAPK has reached the strongest level at 1 mM when primary BMMs were stimulated by RANKL for 15 min. Met pre-incubation for 1 h blocked the phosphorylation of the above proteins. When osteoclasts were stimulated with 5 mM Met, then the phosphorylation of AKT and ERK was gradually decreased with time gradient. These inhibitory effects were similar to those of PI3K/Akt signaling pathway inhibitor LY294002 and MAPK/ERK signaling pathway inhibitor U0126 (Fig. 5).

3. Discussion

Osteoclasts are multinucleated giant cells that are formed by the fusion of many mononuclear osteoclast precursors with myeloid/monocyte sources (Parfitt 2002). The bone resorption capacity of

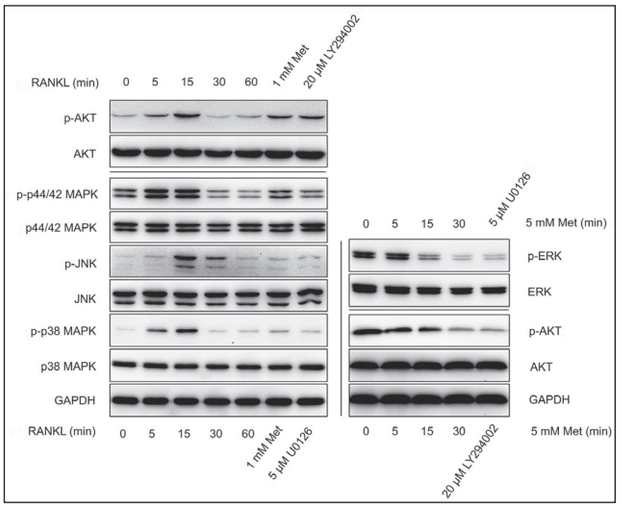

Fig. 5: Metformin regulates osteoclast differentiation and apoptosis through PI3K/Akt signaling pathway, MAPK/ERK signaling pathway and ERK signaling pathway

osteoclasts showed positive correlation with the size of the osteoclasts and the number of nuclei (Lees et al. 2001). Differentiated and mature osteoclasts secrete H^+ into resorption pits through vacuolar ATPases to decompose bone inorganic mineralization components that are dominated by hydroxyapatite. In addition, they can secrete a variety of proteases, such as degradation of extracellular matrix proteins and other collagen-based organic components (Clarke 2008; Väänänen et al. 2000), that are transported into the bone resorption pits through vesicles, and the degradation products of bone matrix are eventually phagocytosed by the osteoclasts. Cathepsin (Cts) and matrix metalloproteinases (MMPs) are the most characteristic related enzymes (Henriksen et al. 2011). In particular, the upregulation of MMP-9 expression during osteoclast differentiation stimulates enhanced bone resorption activity (Andersen et al. 2004). Studies have demonstrated that tetracycline analogues inhibited osteoclast differentiation by inhibiting mmp-9-mediated histone H3 cleavage (Kim et al. 2019). Cytokine receptor activator of nuclear factor kappa B ligand (RANKL) and macrophage colony-stimulating factor (M-CSF) are the key factors for stimulating progenitor cells, which further differentiate into proosteoclasts. Among these, RANKL is mainly involved in inducing osteoclast-specific differentiation process in progenitor cells (Ono et al. 2018; Kim et al. 2002). Nuclear transcription factor-activated T cell 1 (NFATc-1) acts as a key factor in osteoclast differentiation, and studies have confirmed that downregulation of NFATc-1 expression effectively inhibits the formation of osteoclasts (Kim et al. 2015). Specific binding of RANK and RANKL leads activates TRAF6, p38, ERK, and JNK, c-Fos, activator protein-1 (AP-1), and NF-kappa B, resulting in increased expression of NFATc 1 (Kobayashi et al. 2001; Soysa et al. 2012; Lee et al. 2016). This ultimately led to the induction of osteoclast-specific genes, including dendritic cell-specific transmembrane protein (Dcstamp), V-type proton ATPase subunit D2 (Atp6v0d2), acid phosphatase (TRAP), and cathepsin K(Ctsk). These genes showed association with osteoclasts, forming multinucleated giant cells (Soysa et al. 2012; Lee et al. 2006). M-CSF plays an important role in osteoclast proliferation, differentiation, viability and motility (Wang et al. 2018). It has been reported that M-CSF induces RAS/ERK activation by binding to M-CSFR-Tyr559, -Tyr697/Tyr921 and -Tyr973 through SFKs, GRB2 and CBL1, respectively (Alonso et al. 1995; van der Geer et al. 1993; Takeshita et al. 2007; Rohde et al. 2004). Moreover, M-CSF-induced PI3K/AKT activation can be promoted by p85 binding to M-CSF-Tyr721 (Soysa et al. 2012; Lee et al. 2006) and GAB family adaptor proteins (Liu et al. 2001; Lee and States 2000). Akt acts as an important anti-apoptotic factor, and inhibition of Akt activation can lead to increased activation of pro-apoptotic proteins, such as Bcl-2-related X (Bax), Bcl-2-related death promoter (Bad)

and Caspase-3 (Franke et al. 2003). ERK is also an important factor in regulating apoptosis. Studies have confirmed that inhibition of ERK activation can promote phosphorylation of Bcl-2 interacting apoptosis mediator (Bim) and play a role in promoting apoptosis (Sun et al. 2019).

Therefore, primary BMMs from C57 mice were used in this study, which induce osteoclast differentiation with M-CSF and RANKL. Also the low concentration of Met could inhibit osteoclast differentiation and bone resorption function in a dose-dependent manner. Otherwise, high concentrations of Met can promote osteoclast apoptosis along the gradient concentration. An animal model of osteoclast bone destruction was successfully established by injecting osteoclasts into the femoral intercondylar medullary cavity of BALB/C nude mice. Intraperitoneal injection of Met was used as the treatment method to explore the effects of Met on osteoclast bone destruction in animals. The results of micro CT showed that the local bone catabolism was increased after osteoclast injection, and Met could treat this bone destruction. However, if this therapeutic effect is achieved by inhibiting osteoclast differentiation or by promoting osteoclast apoptosis still requires investigation. In order to answer this question, immunohistochemical detection was performed on the femur of nude mice, and confirmed that Met treatment in a dose of 200 mg/kg, which has been selected in our previous experiments, demonstrated dual effects. This not only inhibited the differentiation and formation of osteoclasts, but also promoted osteoclast apoptosis. To further explore the mechanism, we first confirmed that low concentrations of Met could effectively inhibit the expression of TRAP, RANK, Cathepsink, NFATC-1, MMP-9, and TRAF-6 at both gene and protein levels, while high concentrations of Met could increase the expression of Bax and caspase-3, and inhibited the expression of Bcl-2. After that, RANKL, the key factor that promotes osteoclast differentiation, stimulated the primary BMMs within 15 min, and then phosphorylated Akt, p44/42MAPK, JNK, p38MAPK, reaching the strongest level, and 1 mM Met could block the activation of RANKL. When the osteoclasts were stimulated with 5 mM Met, then the phosphorylation of Akt and ERK was shown to be blocked in a time-dependent manner.

In conclusion, low concentrations of Met prevented primary BMMs from fusion and differentiation into mature osteoclasts by blocking the phosphorylation of PI3K/Akt and MAPK/ERK signaling pathways. In addition, high concentrations of Met induced osteoclast apoptosis by blocking the phosphorylation of PI3K/Akt and ERK signaling pathways.

4. Experimental

4.1. Ethics approval

The operation of animal experiments conformed to the animal ethics standards of EU Directive 2010/63/EU for animal experiments. Approval No. 2019168 by the Laboratory Animal Management and Use Committee of Wuhan University.

4.2. Extraction, isolation and culture of primary bone marrow mononuclear cells(BMMs)

The femurs of 4-weeks-old male C57BL/6 mice (Hubei Laboratory Animal Research Center, Wuhan, China) were removed under sterile conditions. The bone marrow cavity was gently rinsed by alpha-MEM (Hyclone, USA) containing 10% FBS (Gibco, USA) and 1% penicillin-streptomycin (Biyuntian, China). The rinsed solution was then filtered through a 200 mesh filter, and quickly incubated at 37 ºC in 5%CO_2 (Thermo, USA), and stood for 24 h. The supernatants were then collected and 50 ng/ml M-CSF (R&D Systems, USA) was added to induce adherence for 3 days.

4.3. Phalloidin staining

The primary BMMs ($2x10^5$ cells per well) were inoculated and 50 ng/ml M-CSF+50 ng/ml RANKL (R&D Systems, USA) was added to induce osteoclast differentiation for 8 days. The primary BMMs were fixed with 4% paraformaldehyde for 20 min, and permeated with 0.5% Tritonx-100 for 5 min, and then incubated with 100 nM phalloidin (Servicebio, China) for 30 min. This was followed by addition of DAPI staining solution (Servicebio, China) for 5 min, and sample imaging under a fluorescence microscope.

4.4. CCK-8 assay for cell proliferation

Primary BMMs ($1x10^4$ cells per well) were inoculated and adherence was within 24 h. Next, different concentrations (0, 0.1, 0.2, 0.5, 1, 2, 5,10 mM) of Met (Adamas, China) were added to stimulate within 48 h. Then, 10 µl CCK-8 solution (Dojindo, Janpa) was added and incubated for 1 h at 37 ºC in 5% CO_2 in dark. The absorbance was measured at 450 nm.

4.5. TRAP Staining

The primary BMMs ($2x10^4$ cells per well) were inoculated and induced for osteoclast differentiation. Meanwhile, Met (0, 0.1, 0.2, and 1 mM) was added to intervene the differentiation process. After 8 days, the osteoclasts were stained according to the operation steps of TRAP staining kit (servicebio, China), and the number of osteoclasts (TRAP positive, with nucleus ≥3) was counted under an inverted microscope (Olympus, Japan).

4.6. Bone resorption lacunae experiment

The primary BMMs ($6x10^4$ cells per well) were inoculated into a 24-well osteo assay plate (Corning, USA), and osteoclast differentiation was induced, while Met (0, 0.1, 0.2, and 1 mM) was used to intervene the differentiation process. After 8 days, the cells were fixed with 4% paraformaldehyde, rinsed with 5% sodium hypochlorite (Sigma-Aldrich, USA), and observed under an inverted microscope (Olympus, Japan). The area was analyzed using image-proplus 6.

4.7. Flow cytometry

The primary BMMs ($1x10^5$ cells per well) were inoculated and osteoclast differentiation was induced. After 8 days, the cells were stimulated with Met (0, 1, 5, and 10 mM) within 24 h. This was followed by operation steps of Annexin V FITC/PI apoptosis kit (MultiSciences, China), and the apoptotic rate was detected by flow cytometry (Backman Coulter, USA).

4.8. Real-time PCR

The primary BMMs ($2x10^5$ cells per well) were inoculated and stimulated by Met (0, 0.1, 0.2, and 1 mM) to intervene osteoclast differentiation for 8 days. In addition, osteoclasts were induced to differentiate for 8 days, and Met (0, 1, 5, and 10 mM) was added for 24 h. Total RNA was extracted according to the instructions of TRIpure Total RNA Extraction Reagent Kit (ELK biotechnology, China). According to the instructions of HiScript III RT SuperMix for qPCR (+gDNA wiper) kit (Vazyme, China), cDNA was obtained by reverse transcription at 50 ºC for 15 min and 85 ºC for 5 s, and the gene expression changes were detected on a q225 fluorescence quantitative qPCR instrument (KUBO, China). The primer sequences were as follows:
GAPDH forward: TGAAGGGTGGAGCCAAAAG;reverse: AGTCTTCTGGGTGGCAGTGAT;
TRAP forward:
TGTTGACAGCGGTCCATCTAG; reverse:AGCGAATCTCCCTGTTCCAC;
RANK forward:
CTCCTTGGAAAGCTAGAAGCAC; reverse: TTCCCTCCCTTCCTGTAGTAAAC;
Cathepsink forward:
GCACCCTTAGTCTTCCGCTC; reverse: GGTCATATAGCCGCCTCCAC;
NFATC-1 forward:
TATATGAGCCCATCCTTGCCT; reverse: GGCTGCCTTCCGTCTCATAG;
MMP-9 forward:
AAAGGCAGCGTTAGCCAGAA; reverse: ACAACTCGTCGTCGTCGAAA;
TRAF6 forward:
CTGTGCTGTGTCCATGGCATAT; reverse: GCAAGTGTCGTGCCAAGTGAT;
Bax forward:
GGGTGGCAGCTGACATGTTT; reverse: GCCTTGAGCACCAGTTTGCT;
bcl-2 forward:
GAGACAGCCAGGAGAAATCA; reverse: CCTGTGGATGACTGAGTACC;
Caspase-3 forward:
TGTCATCTCGCTCTGGTACG; reverse: AAATGACCCCTTCATCACCA;

4.9. Western-blot

Like for the real-time PCR stimulation method, the total protein was extracted with 1:100 ratio of a protease inhibitor Cocktail (MCE, USA):RIPA lysate (Beyotime, China). The protein concentration was then measured according to BCA protein concentration determination kit (Beyotime, China). The protein samples were then prepared, denatured at 100 ºC for 5 min, and loaded. Next, SDS-PAGE electrophoresis was performed and 5% skimmed milk was used for sealing at room temperature within 2 h. The samples were then incubated with primary antibodies overnight in a shaker at 4 ºC, and then incubated with secondary antibodies in a shaker at room temperature for 1 h. The samples underwent ECL development, and the gray values were measured with image J.

4.10. Animal models of osteoclast bone destruction and micro-CT scanning

Six 4-weeks-old male balb/c nude mice (Beijing Sparford Biotechnology Co., Ltd.) were randomly labeled from 1-6. Of these, the first 3 mice were intraperitoneally injected with normal saline (100 µl, twice a week), and the remaining 3 mice were intraperitoneally injected with Met (200 mg/kg, twice a week). The bilateral distal femoral medullary cavities of No. 1 and No. 4 mice were injected with normal saline (30 µl, twice a week); No. 2 and No. 5 were injected with osteoclasts ($5x10^5$ cells/30 µl, twice a week) into the left distal femoral medulla, and saline (30 µl, twice a week) was injected onto the right side; and No. 3 and No. 6 were injected with osteoclasts

($5x10^5$ cells/30 µl, twice a week) into the distal medullary cavity of bilateral femur. Four weeks later, the femurs of nude mice were surgically removed, fixed with tissue fixative solution, and then scanned by micro-CT.

4.11. Immunohistochemical analysis of paraffin sections

The femurs were decalcified by 10% EDTA decalcification solution (Absin, China) at 4 ºC for 3 days at a rotating speed of 0.02 m/s. The femurs were dehydrated by conventional gradient alcohol, and embedded in paraffin at 65 ºC. The paraffin tissues were then sliced (paraffin slicer: Lecia:RM2245) with a thickness of 8 µm, and roasted at 60 ºC for 1 h. After routine dewaxing and hydration, the slices were placed in 1X citric acid repair solution (Servicebio, China), repaired in a microwave oven for 8 min, incubated with 3% H_2O_2 for 5 min, and sealed with 5% BSA (Servicebio, China) for 1 min. The primary antibody (1:200 dilution) was incubated for overnight at 4 ºC, rewarmed at 37 ºC for 30 min, washed with phosphate buffered saline (PBS) followed by biotin-labeled secondary antibody, dripped with SABC reagent (Solarbio, China), and incubated at 37 ºC for 30 min. DAB color was observed, and then was followed by washing with distilled water, restaining with hematoxylin, performing routine dehydration, and dry sealing. The observation was performed by Aperio VERSA 8.

4.12. Western-blot analysis of signal pathways

Primary BMMs ($1x10^6$ cells per well) were inoculated, and stimulated by 50 ng/ml M-CSF and 50 ng/ml RANKL at different time points (0, 5, 15, 30, and 60 min), and three other dishes of cells were pre-incubated with 1 mM Met, 20 mM LY294002 (MCE, USA), and 5 mM U0126 (MCE, USA) for 1 h. The 50 ng/ml M-CSF and 50 ng/ml RANKL were then added to stimulate the cells for 15 min. In addition, osteoclasts were differentiated for 8 days, stimulated with 5 mM Met at different time points (0, 5, 15, 30 min), and stimulated with 20 µM LY294002 and 5 µM U0126for 30 min as positive control groups. As in the previous western blotting steps, the ECL chemiluminescence imaging system (TANON-5200) was applied to analyze the changes in the protein expression.

4.13. Statistical analysis

All experimental studies were repeated at least 3 times, and the data were expressed as means ± standard deviation. T-test was performed to compare the differences between the two groups. $P<0.05$ was defined as statistically different, and $P<0.01$ as significant difference.

Conflicts of interest: none declared.

References

Alonso G, Koegl M, Mazurenko N, Courtneidge SA (1995) Sequence requirements for binding of Src family tyrosine kinases to activated growth factor receptors. J Biol Chem 270: 9840–9848.

Andersen TL, del Carmen Ovejero M, Kirkegaard T, Lenhard T, Foged NT, Delaissé JM (2004) A scrutiny of matrix metalloproteinases in osteoclasts: evidence for heterogeneity and for the presence of MMPs synthesized by other cells. Bone 35: 1107–1119.

Bansal M, Siegel E, Govindarajan R (2011) The effect of metformin (M) on overall survival (OS) of patients (Pts) with colorectal cancer (CRC) treated with chemotherapy (CTX). J Clin Oncol 29: 2696–2696.

Boyle WJ, Simonet WS, Lacey DL (2003) Osteoclast differentiation and activation. Nature 423: 337–342.

Clarke B (2008) Normal bone anatomy and physiology. Clin J Am Soc Nephrol 3 Suppl 3: S131–139.

Dziedzic A, Saluk-Bijak J, Miller E, Bijak M (2020) Metformin as a potential agent in the treatment of multiple sclerosis. Int J Mol Sci 21: 5957.

Franke TF, Hornik CP, Segev L, Shostak GA, Sugimoto C: PI3K/Akt and apoptosis: size matters. Oncogene 22: 8983–8998.

Henriksen K, Bollerslev J, Everts V, Karsdal MA (2011) Osteoclast activity and subtypes as a function of physiology and pathology--implications for future treatments of osteoporosis. Endocr Rev 32: 31–63.

Kim KJ, Yeon JT, Choi SW, Moon SH, Ryu BJ, Yu R, Park SJ, Kim SH, Son YJ (2015) ecursin inhibits osteoclastogenesis by downregulating NFATc1 and blocking fusion of pre-osteoclasts. Bone 81: 208–216.

Kim N, Takami M, Rho J, Josien R, Choi Y (2002) A novel member of the leukocyte receptor complex regulates osteoclast differentiation. J Exp Med 195: 201–209.

Kim Y, Kim J, Lee H, Shin WR, Lee S, Lee J, Park JI, Jhun BH, Kim YH, Yi SJ, Kim K (2019) Tetracycline analogs inhibit osteoclast differentiation by suppressing MMP-9-mediated histone H3 cleavage. Int J Mol Sci 20: 4038.

Kobayashi N, Kadono Y, Naito A, Matsumoto K, Yamamoto T, Tanaka S, Inoue J (2001) Segregation of TRAF6-mediated signaling pathways clarifies its role in osteoclastogenesis. Embo J 20: 1271–1280.

Lee AW, States DJ (2000) Both src-dependent and -independent mechanisms mediate phosphatidylinositol 3-kinase regulation of colony-stimulating factor 1-activated mitogen-activated protein kinases in myeloid progenitors. Mol Cell Biol 20: 6779–6798, 2000.

Lee K, Chung YH, Ahn H, Kim H, Rho J, Jeong D (2016) Selective regulation of MAPK signaling mediates RANKL-dependent osteoclast differentiation. Int J Biol Sci 12: 235–245.

Lee SH, Rho J, Jeong D, Sul JY, Kim T, Kim N, Kang JS, Miyamoto T, Suda T, Lee SK, Pignolo RJ, Koczon-Jaremko B, Lorenzo J, Choi Y (2006) v-ATPase V0 subunit d2-deficient mice exhibit impaired osteoclast fusion and increased bone formation. Nat Med 12: 1403–1409.

Lees RL, Sabharwal VK, Heersche JN (2001) Resorptive state and cell size influence intracellular pH regulation in rabbit osteoclasts cultured on collagen-hydroxyapatite films. Bone 28: 187–194.

Libby G, Donnelly LA, Donnan PT, Alessi DR, Morris AD, Evans JM (2009) New users of metformin are at low risk of incident cancer: a cohort study among people with type 2 diabetes. Diabetes Care 32: 1620–1625.

Liu Y, Jenkins B, Shin JL, Rohrschneider LR (2001) Scaffolding protein Gab2 mediates differentiation signaling downstream of Fms receptor tyrosine kinase. Mol Cell Biol 21: 3047–3056.

Melton LJ, 3rd, Leibson CL, Achenbach SJ, Therneau TM, Khosla S (2008) Fracture risk in type 2 diabetes: update of a population-based study. J Bone Miner Res 23: 1334–1342.

Ono T, Nakashima T (2018) Recent advances in osteoclast biology. Histochem Cell Biol 149: 325–341.

Parfitt AM (2002) High bone turnover is intrinsically harmful: two paths to a similar conclusion. The Parfitt view. J Bone Miner Res 17: 1558–1559; author reply 1560.

Rohde CM, Schrum J, Lee AW (2004) A juxtamembrane tyrosine in the colony stimulating factor-1 receptor regulates ligand-induced Src association, receptor kinase function, and down-regulation. J Biol Chem 279: 43448–43461.

Soysa NS, Alles N, Aoki K, Ohya K (2012) Osteoclast formation and differentiation: an overview. J Med Dent Sci 59: 65–74.

Sun QY, Ding LW, Johnson K, Zhou S, Tyner JW, Yang H, Doan NB, Said JW, Xiao JF, Loh XY, Ran XB, Venkatachalam N, Lao Z, Chen Y, Xu L, Fan LF, Chien W, Lin DC, Koeffler HP (2019) SOX7 regulates MAPK/ERK-BIM mediated apoptosis in cancer cells. Oncogene 38: 6196–6210.

Takeshita S, Faccio R, Chappel J, Zheng L, Feng X, Weber JD, Teitelbaum SL, Ross FP (2007) c-Fms tyrosine 559 is a major mediator of M-CSF-induced proliferation of primary macrophages. J Biol Chem 282: 18980–18990.

Väänänen HK, Zhao H, Mulari M, Halleen JM (2000) The cell biology of osteoclast function. J Cell Sci 113: 377–381.

van der Geer P, Hunter T (1993) Mutation of Tyr697, a GRB2-binding site, and Tyr721, a PI 3-kinase binding site, abrogates signal transduction by the murine CSF-1 receptor expressed in Rat-2 fibroblasts. Embo J 12: 5161–5172.

Wang L, Iorio C, Yan K, Yang H, Takeshita S, Kang S, Neel BG, Yang W (2018) A ERK/RSK-mediated negative feedback loop regulates M-CSF-evoked PI3K/AKT activation in macrophages. Faseb J 32: 875–887.

Xu H, Chen K, Jia X, Tian Y, Dai Y, Li D, Xie J, Tao M, Mao Y (2015) Metformin use is associated with better survival of breast cancer patients with diabetes: a meta-analysis. Oncologist 20: 1236–1244.